Kinetics and Mechanism of the O Atom Reaction with Dimethyl Sulfoxide

ARTICLE *in* THE JOURNAL OF PHYSICAL CHEMISTRY A · JULY 2003

Impact Factor: 2.69 · DOI: 10.1021/jp0226127

Kinetics and Mechanism of the O Atom Reaction with Dimethyl Sulfoxide

Véronique Riffault, Yuri Bedjanian,* and Georges Le Bras

Laboratoire de Combustion et Systèmes Réactifs,CNRS, and Université d'Orléans, 45071 Orléans Cedex 2, France

Received: December 17, 2002; In Final Form: April 30, 2003

The kinetics and mechanism of the reaction O + DMSO → products (1) have been studied by the mass spectrometric discharge-flow method at 298 K and at a total pressure of 1 Torr of helium. The reaction rate coefficient was measured under pseudo-first-order conditions either from the kinetics of O atom consumption in excess of DMSO or from the kinetics of DMSO decay in excess of O atoms: $k_1 = (1.0 \pm 0.2) \times 10^{-11}$ $cm^3 molecule^{-1} s^{-1}$ (uncertainty includes 2σ statistical error and estimated systematic errors). Both CH_3 and SO_2 were detected as the products of reaction 1, and the reaction O + DMSO → $2CH_3$ + SO_2 was found to be the main (if not unique) channel of reaction 1 under the experimental conditions of the study. This result indicates that reaction 1 cannot be a suitable laboratory source of the atmospheric relevant CH_3SO_2 radical, at least at low pressures. In addition, the upper limits, $k_3 < 1 \times 10^{-13}$ and $k_4 < 5 \times 10^{-15}$ cm^3 $molecule^{-1}$ s^{-1}, were determined for the rate coefficients of the reactions CH_3 + DMSO → products (3) and Br_2 + DMSO → products (4), respectively. The rate constant of the self-combination of CH_3 radicals, $CH_3 + CH_3$ (+M) → C_2H_6 (+M) (2), was also determined in the pressure range between 0.5 and 3.0 Torr of He.

Introduction

Largely emitted by oceans, dimethyl sulfide (DMS) is involved in the global climate system through the formation of aerosols and clouds which might significantly influence the earth radiation budget.[1] Dimethyl sulfoxide (DMSO) has been observed in marine atmosphere [e.g., ref 2−4] and is a key intermediate species in DMS oxidation [e.g., ref 5]. Atmospheric DMSO is mainly produced by the addition pathway of the OH reaction with DMS [e.g., ref 6]. The BrO + DMS reaction which has been found to stoichiometrically produce DMSO[7−9] may also contribute to atmospheric DMSO. Despite the importance of DMSO in the atmospheric sulfur chemistry, the gas-phase reactions of this species have not been much studied so far. One of the reasons seems to be the experimental difficulties with DMSO handling due to low vapor pressure of this species and its "stickiness". One of the few elementary reactions of DMSO studied is the reaction with OH radicals. In addition to rate constant measurements,[10] a mechanistic study, using time-resolved tunable laser absorption spectroscopy detection of methyl radicals, has yielded a near unity CH_3 yield in the OH + DMSO reaction.[10] The reaction mechanism suggested includes energized OH-DMSO adduct formation followed by CH_3 elimination. If a similar CH_3 elimination mechanism is supposed for the reaction of O atoms with DMSO, one can expect the formation of the CH_3SO_2 radical as the coproduct of this reaction. The CH_3SO_2 radical is a potentially important intermediate in the atmospheric DMS oxidation. There is evidence that this radical is produced in the OH abstraction pathway of DMS oxidation [e.g., ref 11]. This radical has also been suggested to be formed in the OH-addition channel of DMS oxidation from the OH + $CH_3S(O)OH$ reaction, $CH_3S(O)OH$ being the coproduct of CH_3 in the OH + DMSO reaction.[10] Information on the stability and chemical reactivity of the CH_3SO_2 radical is therefore of great importance. In this respect, the O + DMSO reaction could be a convenient source of this radical for laboratory studies.

* To whom correspondence should be addressed. E-mail: bedjanian@cnrs-orleans.fr.

The present paper reports the results of the experimental study of the kinetics and products of the reaction 1 at room temperature and 1 Torr total pressure of helium

$$O + DMSO \rightarrow \text{products} \quad (1)$$

When this paper was in preparation, the results of another kinetic study of reaction 1 were reported.[12] In that study, the reaction rate constant was measured as a function of temperature (266−383 K) and pressure (20−100 Torr of N_2); however, the primary reaction products remain unknown.

The following reactions were also investigated as a part of the present study:

$$CH_3 + CH_3\ (+M) \rightarrow C_2H_6\ (+M) \quad (M = He,\ P = 0.5 - 3.0\ Torr) \quad (2)$$

$$CH_3 + DMSO \rightarrow \text{products} \quad (3)$$

$$Br_2 + DMSO \rightarrow \text{products} \quad (4)$$

Methyl radicals were detected as products of reaction 1, and consequently, the information on possible secondary reactions 2 and 3 was needed for the determination of the CH_3 yield from reaction 1. Br_2 was added to the reactive system in order to indirectly detect CH_3 (see the Experimental Section), so that information on its reaction with DMSO was also needed.

Experimental Section

Experiments were carried out in a discharge flow reactor using a modulated molecular beam mass spectrometer as the detection method. The main reactor, shown in Figure 1 along with the movable injector for the reactants, consisted of a Pyrex tube (45 cm length and 2.4 cm i.d.). The walls of the reactor and of the injector were coated with halocarbon wax in order to minimize the heterogeneous loss of active species. All experiments except those for $CH_3 + CH_3$ reaction were conducted at $T = 298$ K and 1 Torr total pressure, with helium being used as the carrier gas.

10.1021/jp0226127 CCC: $25.00
Published on Web 06/24/2003

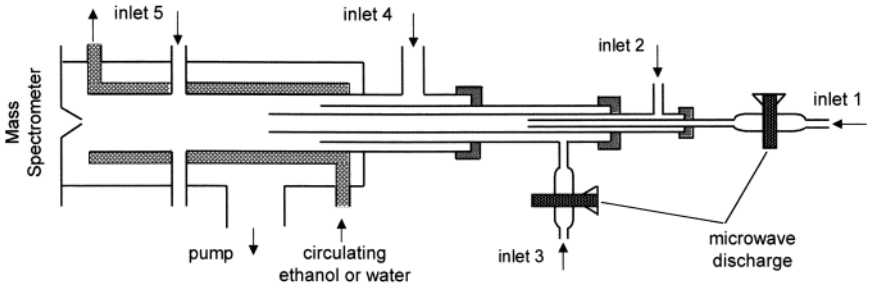

Figure 1. Diagram of the apparatus used.

Oxygen atoms were generated from the microwave discharge in O_2/He mixtures introduced through inlet 1. Two detection methods of O atoms were used. First, at high concentrations of oxygen atoms, O was detected at its parent peak as O^+ (m/e = 16). Two methods were used in this case for determination of the absolute concentrations of the atoms: the first one used the fraction of O_2 dissociated in the microwave discharge ([O] = $2\Delta[O_2]$), whereas the second one used the reaction of excess oxygen atoms with NO_2 ($\Delta[O] = \Delta[NO_2]$):

$$O + NO_2 \rightarrow NO + O_2 \quad (5)$$

$$k_5 = 9.7 \times 10^{-12}\ \text{cm}^3\ \text{molecule}^{-1}\ \text{s}^{-1}\ ^{13}$$

(all rate constants are given at T = 298K).

In the last case, the secondary reaction 6 is too slow to influence the results of the calibration experiments:

$$O + NO\ (+M) \rightarrow NO_2\ (+M) \quad (6)$$

$$k_6 = 9.0 \times 10^{-32}\ \text{cm}^6\ \text{molecule}^{-2}\ \text{s}^{-1}\ ^{13}$$

The results obtained by these two calibration methods were always in good agreement (within 5%).

At low concentrations of the oxygen atoms, Br_2 was added at the end of the reactor through inlet 5 (located 5 cm upstream of the sampling cone) in order to titrate O atoms:

$$O + Br_2 \rightarrow BrO + Br \quad (7)$$

$$k_7 = 2.0 \times 10^{-11}\ \text{cm}^3\ \text{molecule}^{-1}\ \text{s}^{-1}\ ^{14}$$

Thus, O was detected as BrO^+ (m/e = 95/97). BrO was calibrated by chemical conversion of BrO to NO_2 through reaction 8 in excess of NO (inlet 5) with subsequent detection of NO_2 formed ($[BrO]_0 = [NO_2]_{formed}$):

$$BrO + NO \rightarrow Br + NO_2 \quad (8)$$

$$k_8 = 2.1 \times 10^{-11}\ \text{cm}^3\ \text{molecule}^{-1}\ \text{s}^{-1}\ ^{13}$$

In this case, BrO was formed through reaction 7 in excess of Br_2 (inlet 4). In these calibration experiments, the recombination reaction of BrO radicals (9) was negligible due to the high NO and low BrO concentrations used:

$$BrO + BrO \rightarrow \text{products} \quad (9)$$

$$k_9 = 3.2 \times 10^{-12}\ \text{cm}^3\ \text{molecule}^{-1}\ \text{s}^{-1}\ ^{13}$$

DMSO was injected into the reactor through inlet 4 through a continuous flow of He bubbling in liquid DMSO and detected at its parent peak as $DMSO^+$ (m/e = 78). The measurement of the absolute concentrations of DMSO in the flow reactor represents a significant experimental challenge because of the low vapor pressure of DMSO (ca 0.6 Torr at 298 K) and its sticky behavior. DMSO losses in the flow tubing are usually observed (e.g., ref 10). In this work, a new in situ method to determine DMSO concentrations in laboratory studies is proposed. This direct calibration method uses the title reaction O + DMSO → 2 CH_3 + SO_2 (mechanistic information from this study is given below) and consists of the chemical conversion of DMSO to SO_2 which can be easily calibrated ($\Delta[DMSO] = \Delta[SO_2]$). Figure 2 presents an example of the calibration plot: the dependence of the consumed concentration of DMSO vs concentration of SO_2 formed (m/e = 64). It can be noticed that the concentrations have been varied over a wide range (about 60 times) and that there is an excellent agreement between the results obtained in excess of O atoms, when DMSO was completely removed ($[DMSO]_0 = [SO_2]_{formed}$), and those in excess of DMSO, when the concentration of SO_2 formed was equal to the consumed fraction of DMSO ($\Delta[DMSO] = [SO_2]_{formed}$). In these calibration experiments, possible secondary reactions are too slow to influence the results:

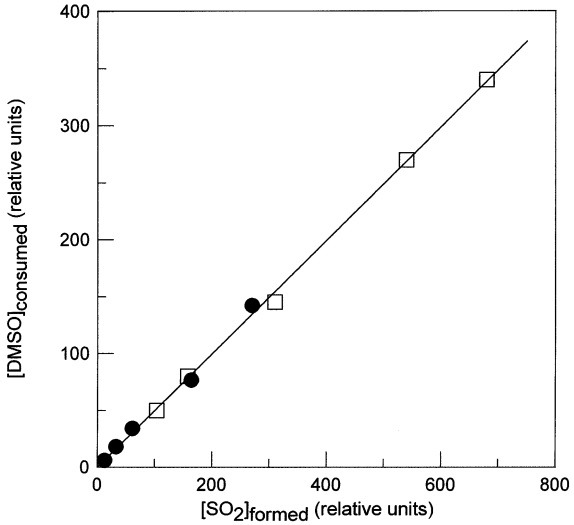

Figure 2. Dependence of the consumed concentration of DMSO (signal intensity at m/e = 78) on the concentration of SO_2 formed (signal intensity at m/e = 64). Results obtained in excess of O atoms (●) and in excess of DMSO (□).

$$O + SO_2\ (+M) \rightarrow SO_3\ (+M) \quad (10)$$

$$k_{10} = 1.3 \times 10^{-33}\ \text{cm}^6\ \text{molecule}^{-2}\ \text{s}^{-2}\ ^{13}$$

$$CH_3 + SO_2 \rightarrow \text{products} \quad (11)$$

$$k_{11} = 2.9 \times 10^{-13}\ \text{cm}^3\ \text{molecule}^{-1}\ \text{s}^{-1}\ (P = 50-200\ \text{Torr of argon})^{15}$$

The reaction of H atoms (produced from the O + CH_3 reaction)

with SO_2 is also relatively slow:

$$O + CH_3 \rightarrow H + CH_2O \quad (12)$$

$$k_{12} = 1.1 \times 10^{-10}\ cm^3\ molecule^{-1}\ s^{-1}\ ^{13}$$

$$H + SO_2\ (+M) \rightarrow HSO_2\ (+M) \quad (13)$$

$$k_{13} < 1.4 \times 10^{-33}\ cm^6\ molecule^{-2}\ s^{-1}\ ^{16}$$

Anyway, no SO_2 consumption was observed at highest reaction times when DMSO was already consumed, however O atoms were still present in the reactor.

In all experiments, CH_3 was detected as CH_3Br^+ at m/e = 94/96, after scavenging by an excess of Br_2 (added at the end of the reactor through inlet 5). Thus, CH_3 was converted into CH_3Br via reaction 14:

$$CH_3 + Br_2 \rightarrow CH_3Br + Br \quad (14)$$

$$k_{14} = 3.9 \times 10^{-11}\ cm^3\ molecule^{-1}\ s^{-1}\ ^{17}$$

This method of CH_3 detection was preferred to the direct monitoring of the signal at m/e = 15 (CH_3^+) because of the significant contribution of DMSO at this mass. The method used for the CH_3 detection implies that secondary reactions resulting from Br_2 addition into the reactive system are negligible. As Br_2 was added into the reactor only in the experiments carried out in excess of DMSO, the potentially important secondary reactions to be considered are those of DMSO with Br_2 and with Br atoms, which are formed as coproduct of CH_3Br in reaction 14:

$$DMSO + Br_2 \rightarrow \text{products} \quad (4)$$

$$DMSO + Br \rightarrow \text{products} \quad (15)$$

Reaction 4 was studied in the present work (see below) and was found to be very slow. Reaction 15 was recently investigated using a relative rate method.[18] The value of $k_{15} = (2.4 \pm 1.6) \times 10^{-14}$ cm^3 molecule^{-1} s^{-1} was measured at T = 298 K and P = 740 Torr. With this rate constant and the one for reaction 4 (see below), reactions 4 and 15 are negligible under the experimental conditions of the present study. Absolute concentrations for CH_3Br and the other molecular species used in the study were determined directly from their flow rates, obtained from measurements of the pressure drop in calibrated volume flasks containing known mixtures of the species with Helium.

The purities of the gases used were as follows: He > 99.9995% (Alphagaz), was passed through liquid nitrogen traps; DMSO > 99.9% (Adrich); Br_2 > 99.99% (Aldrich); CH_3Br > 99.5% (UCAR); O_2 > 99.995% (Alphagaz); SO_2 > 99.9% (Alphagaz); NO_2 > 99% (Alphagaz); NO > 99% (Alphagaz), purified by trap-to trap distillation in order to remove NO_2 traces.

Results

Rate Constant of the O + DMSO Reaction. Two series of experiments were performed to measure the rate constant of the reaction O + DMSO: the first one by monitoring DMSO consumption kinetics in excess of O atoms and the second one by monitoring O concentration decays in excess of DMSO.

DMSO Kinetics in Excess of O Atoms. The kinetics of reaction 1 was first determined in excess of O atoms, with DMSO being injected by inlet 4 and O produced from the microwave discharge (inlet 1) and detected at m/e = 16. Initial concentrations were in the following ranges: $[DMSO]_0 = (2-7) \times 10^{11}$ molecule cm^{-3} and $[O]_0 = (0.4-5.1) \times 10^{13}$ molecule cm^{-3}. Flow velocities in the reactor were 1140−1750 cm s^{-1}. The experiments were carried out under pseudo-first-order conditions and O consumption was observed to be negligible. Figure 3 shows examples of exponential decays of [DMSO] for various concentrations of oxygen atoms in excess. The pseudo-first-order rate constants, $k_1' = -d(\ln[DMSO])/dt$, were corrected for the axial and radial diffusion of DMSO.[19] The diffusion coefficient of DMSO in He was taken as similar to that of Kr in He[20] and was calculated to be equal to 0.65 atm cm^2 s^{-1} at T = 298 K. These corrections on the measured values of k_1' were up to 18% for a few kinetic runs, however, generally less than 10%. The pseudo-first-order plot measured from DMSO decay kinetics in excess of O atoms is shown in Figure 4. The linear least-squares fit to these experimental data provides the following value for the rate coefficient of reaction 1:

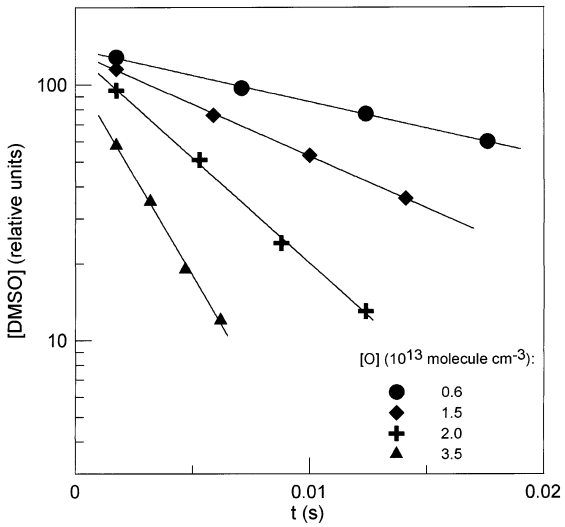

Figure 3. Reaction O + DMSO: example of experimental DMSO decays in excess of O atoms.

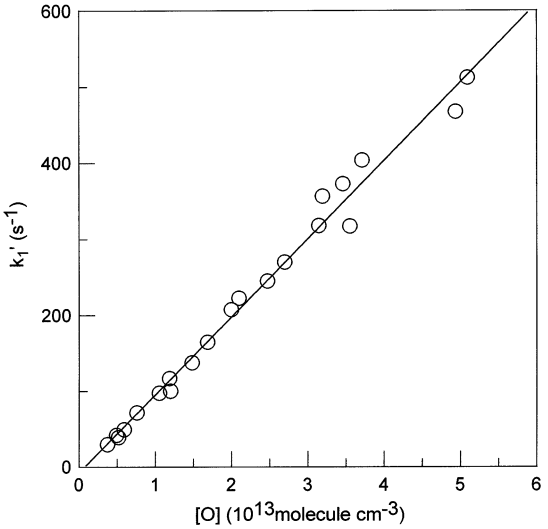

Figure 4. Reaction O + DMSO: pseudo-first-order plot obtained from DMSO decay kinetics in excess of O atoms.

$$k_1 = (1.03 \pm 0.03) \times 10^{-11}\ cm^3\ molecule^{-1}\ s^{-1}$$

(where the uncertainty represents 1σ). The zero-intercept, in the range $-(7.4 \pm 7.2)$ s^{-1}, is in good agreement with the

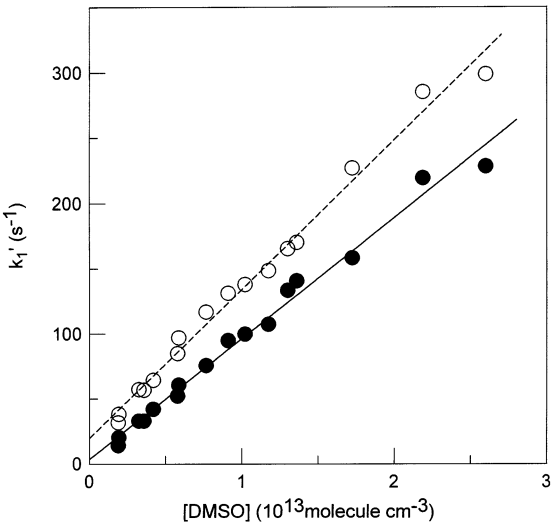

Figure 5. Reaction O + DMSO: pseudo-first-order plot obtained from O decay kinetics in excess of DMSO. (○) data obtained from the simple exponential fit to experimental kinetics; (●) data corrected for the contribution of the O + CH_3 reaction (see text).

experimental observation that no change in DMSO concentrations was observed in the absence of O atoms when the injector was moved.

O Atoms Kinetics in Excess of DMSO. A second series of experiments were performed in excess of DMSO, monitoring O atom decays under pseudo-first-order conditions. The reactants were injected in the same way as in the first series of experiments, but O atoms were detected as BrO (see the Experimental Section). This detection method of O atoms implies that the concentrations of BrO formed in reaction 7 are not influenced by possible reactions of BrO with excess DMSO:

$$\mathrm{BrO} + \mathrm{DMSO} \rightarrow \text{products} \qquad (16)$$

$$k_{16} = (1.0 \pm 0.3) \times 10^{-14}\ \mathrm{cm^3\ molecule^{-1}\ s^{-1}}$$ [18]

Considering this value and the range of the DMSO concentrations used in these experiments ($[DMSO]_0 = (0.2-2.6) \times 10^{13}$ molecule cm^{-3}), the possible effect of reaction 16 on measured BrO concentrations can be neglected. The concentrations of the oxygen atoms were in the range: $[O]_0 = (2.7-3.9) \times 10^{11}$ molecule cm^{-3}. The concentrations of Br_2, added at the end of the reactor (inlet 5), were always around 5×10^{13} molecule cm^{-3}. Flow velocities in the reactor were 1000−1100 cm s^{-1}. Under these experimental conditions, DMSO consumption was observed to be negligible (less than 5%). Pseudo-first-order rate constants, $k_1' = -\mathrm{d}(\ln[O])/\mathrm{d}t$, obtained from O atom kinetics, were corrected for axial and radial diffusion of O atoms. The diffusion coefficient of O in He used in these calculations was 1.07 atm cm^2 s^{-1} at 298 K.[21] The diffusion corrections on measured values of k_1' were up to 17%, though generally less than 10%. Under the experimental conditions used in this series of experiments, the secondary reaction 12 between O atoms and CH_3 radicals produced in the reaction O + DMSO (see below) cannot be avoided and has to be taken into account. The experimental kinetic runs were simulated using a simple mechanism including reaction 1 forming two CH_3 radicals and SO_2 (see below) and secondary reaction 12. Figure 5 presents the pseudo-first-order plots obtained from the simple exponential fit to the experimental kinetics of O atom consumption and the data corrected for the contribution of reaction 12. Corrections on k_1' were less important for the highest DMSO concentrations (around 17%) than for the lowest ones (up to 55%). It can be also noted that the slope of the linear fit to the simulated points in Figure 5, which provides the value of the rate constant for reaction 1, is not significantly affected by the corrections on the experimental data points. For example, the difference between the values of k_1 resulting from the two fits presented in Figure 5 is around 20%. Finally, the value

$$k_1 = (0.93 \pm 0.03) \times 10^{-11}\ \mathrm{cm^3\ molecule^{-1}\ s^{-1}}$$

could be derived from these experiments (the uncertainty corresponds to 1σ). The intercept (3.5 ± 3.4) s^{-1} is in agreement with the negligible decay of O atoms experimentally observed in the absence of DMSO in the reactor.

The value of k_1 determined in this series of experiments is in good agreement with that obtained above from the monitoring of DMSO consumption kinetics in excess of O atoms. The final value of k_1, which can be recommended from this work is

$$k_1 = (1.0 \pm 0.2) \times 10^{-11}\ \mathrm{cm^3\ molecule^{-1}\ s^{-1}} \text{ at } T = 298\ \mathrm{K}$$

The uncertainties on k_1 represent a combination of statistical and estimated systematic errors. The estimated systematic uncertainties include ±5% for flow meter calibrations, ±3% for pressure measurements, and ±15% for the measurements of the absolute concentrations of the species involved. Combining these uncertainties in quadrature and adding 2σ (∼6%) statistical uncertainty (see Table 1), yields ∼20% overall uncertainty on the value of k_1.

TABLE 1: Reaction $CH_3 + CH_3$ (+M) → C_2H_6 (+M): Experimental Conditions and Results

pressure (Torr of He)	no./ runs	$[CH_3]_0$ (10^{12} molecule cm^{-3})	k_2[a] (10^{-11} cm^3molecule$^{-1}s^{-1}$)
0.5	14	0.2−4.8	2.4 ± 0.4
1.0	11	0.5−4.6	3.0 ± 0.5
3.0	7	0.6−7.2	3.5 ± 0.6

[a] The uncertainty represents a combination of the statistic and estimated systematic errors.

Products of the O + DMSO Reaction. Two series of experiments were conducted to determine the mechanism of reaction 1. The first one consisted of the measurements of the concentrations of SO_2 and CH_3 formed in reaction 1 as a function of the consumed concentration of oxygen atoms. Relatively short reaction times (typically 2.5−3 ms) and high DMSO concentrations (∼5×10^{13} molecule cm^{-3}) were used in these experiments in order to minimize the influence of secondary reactions on the detected concentrations of CH_3 and SO_2. Br_2 (∼2×10^{14} molecule cm^{-3}) was added through inlet 5, so that O was detected as BrO and CH_3 as CH_3Br (see the Experimental Section). For a fixed reaction time and an initial DMSO concentration, the initial O atom concentration, $[O]_0$, was varied and its consumption was measured, as well as the formed concentration of both products. The results presented in Figure 6 show that there is no linear dependence between consumed O atom concentration and the concentration of products formed. The reason for this is that the fast secondary reactions O + CH_3 (12) and $CH_3 + CH_3$ (2) cannot be made negligible, and they (especially reaction 12) influence significantly the yield of the products. The dashed line in Figure 6 represents a yield of unity for SO_2 formation. One can note that, for low $[O]_{consumed}$ (corresponding to low initial concentrations of O atoms), the influence of secondary reactions on concentration of SO_2 is negligible and the SO_2 yield is near unity. The influence of reaction 12 on the measured CH_3

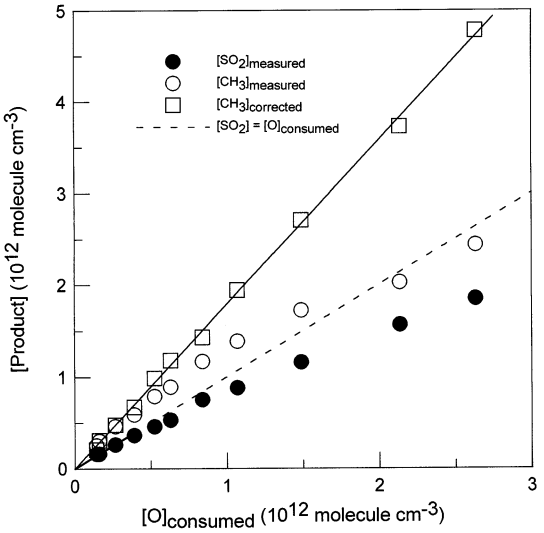

Figure 6. Reaction O + DMSO: measured and corrected concentrations of SO_2 and CH_3 formed in reaction 1 as a function of consumed concentration of O atoms.

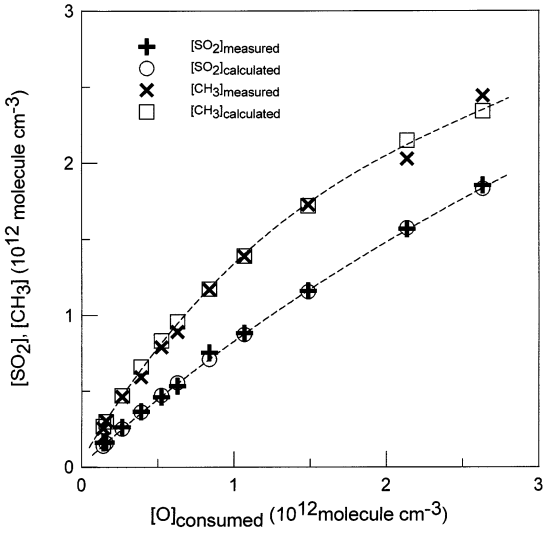

Figure 7. Reaction O + DMSO: measured and simulated concentrations of SO_2 and CH_3 formed in reaction 1 as a function of consumed concentration of O atoms.

concentrations can be easily accounted for without any numerical simulation. Actually, if each O atom consumed in reaction 1 produces one SO_2 molecule, then the difference between $[SO_2]_{measured}$ and $[O]_{consumed}$ is due to O consumption in reaction 12. Thus, the O atom concentration consumed in the secondary reaction with CH_3 can be written as $[O]_{consumed} - [SO_2]_{measured}$ (the difference between the dashed line and the filled circles in Figure 6). Then, considering that each of these O atoms which consumes one CH_3 radical in reaction 12 does not produce two CH_3 radicals in reaction 1, the concentration of CH_3 corrected for the secondary reaction 12 can be expressed as

$$[CH_3]_{corrected} = [CH_3]_{measured} + 3([O]_{consumed} - [SO_2]_{measured})$$

The results of this calculation are presented in Figure 6. The continuous line represents the linear through origin fit to these corrected data and provides the ratio $[CH_3]_{formed}/[O]_{consumed} = 1.80 \pm 0.05$ (1σ), in good agreement with the channel O + DMSO $\rightarrow 2CH_3 + SO_2$ which was assumed for reaction 1. The results of another approach to the treatment of experimental data are shown in Figure 7. In this case, the concentrations of SO_2 and CH_3 were simulated using a reaction mechanism including reaction 1 forming $2CH_3 + SO_2$, reaction 12 and reaction 2. The wall loss processes of O atoms and CH_3 radicals were considered to be negligible compared with the fast gas-phase chemistry. One can note an excellent agreement (within 10%) between the experimental concentrations of products and those calculated with the branching ratio of unity for the $SO_2 + 2CH_3$ channel of reaction 1.

In another series of experiments, the kinetics of O consumption was monitored simultaneously with the kinetics of CH_3 and SO_2 formation. A typical example of the experimental results is shown in Figure 8, where $[O]_0 = 3.35 \times 10^{11}$ molecule cm^{-3} and $[DMSO]_0 = 1.5 \times 10^{13}$ molecule cm^{-3}. The numerical simulation included reactions 1, 2, and 12. For reaction 1, the $2CH_3 + SO_2$ forming channel was considered and the rate constant was varied to fit the O experimental profile. For the example presented in Figure 8, the best fit was obtained with $k_1 = 8.5 \times 10^{-12}$ $cm^3 molecule^{-1} s^{-1}$, in good agreement with the value of k_1 presented above.

Thus, the results obtained in the mechanistic study of reaction 1 imply a unity branching ratio for the $2CH_3 + SO_2$ forming channel of this reaction.

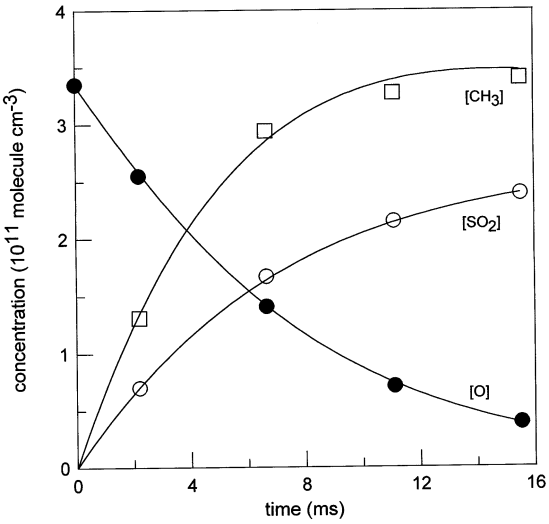

Figure 8. Reaction O + DMSO: example of experimental (points) and simulated (lines) kinetics for O, SO_2, and CH_3.

Rate Constant of the $CH_3 + CH_3$ Reaction. Reaction 2 between methyl radicals was studied as a part of this work, because no kinetic data are available at 1 Torr pressure of He, and this reaction appeared to be an important secondary reaction in the study of reaction 1. Experiments were carried out in the pressure range (0.5−3.0) Torr. Flow velocities ranged from 840 to 1100 cm s^{-1}. CH_3 radicals were formed in the reaction between F (produced by the dissociation of F_2/He mixture in the microwave discharge; inlet 3) and methane (inlet 4):

$$F + CH_4 \rightarrow HF + CH_3 \qquad (17)$$

$$k_{17} = 6.7 \times 10^{-11} \text{ cm}^3 \text{ molecule}^{-1} \text{ s}^{-1}$$ [13]

It was verified by mass spectrometry that more than 90% of F_2 was dissociated in the microwave discharge. To reduce F atom reactions with the glass surface inside the microwave cavity, a ceramic (Al_2O_3) tube was inserted in this part of the injector. This source of F atoms is known to produce O atoms also. The concentrations of the trace O atoms formed in the discharge of F_2 could be easily measured by adding Br_2 into the reactor (inlet 5) and detecting O as BrO^+ ($m/e = 95/97$). CH_3 was converted

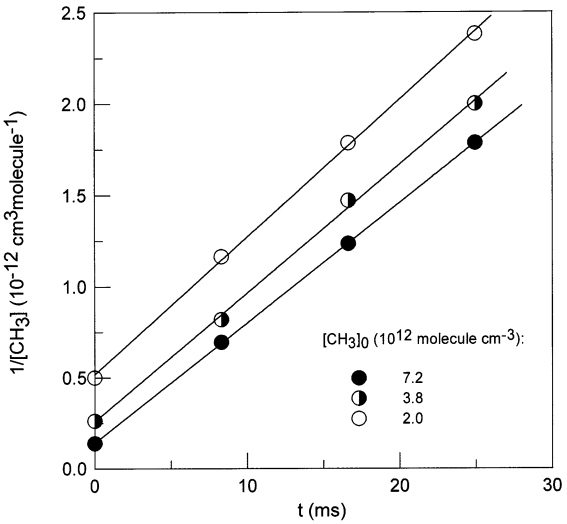

Figure 9. Reaction $CH_3 + CH_3$ (+M): example of kinetic runs at $P = 3.0$ Torr for different initial concentrations of CH_3.

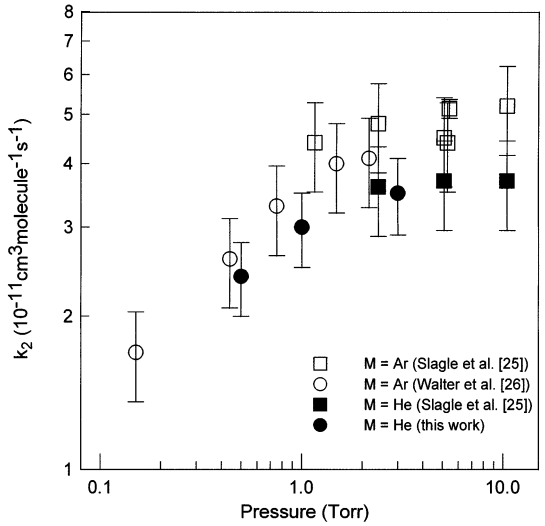

Figure 10. Reaction $CH_3 + CH_3$ (+M): summary of the available rate constant data at $P \leq 10$ Torr of He and Ar.

to CH_3Br through reaction 14 and detected as CH_3Br^+ at $m/e = 94/96$.

The observed consumption of CH_3 was due to reaction 2 and, to a lesser extent, the wall loss of CH_3 radicals and reaction 12 as low O atom concentrations from the F_2 discharge were measured. These O atom concentrations were generally less than 5% of $[CH_3]_0$; however, they reached up to 20% of $[CH_3]_0$ at the lowest initial concentrations of the CH_3 radicals. The rate constant of reaction 2 was derived from the simulation of the experimental kinetics of CH_3 consumption using the mechanism including reactions 2 and 12. The CH_3 wall loss (≤ 1.5 s^{-1}) was negligible compared with CH_3 consumption in the gas phase. Figure 9 presents an example of CH_3 decay kinetics for different initial concentrations of the radicals. One can note that the plots of $1/[CH_3]$ versus reaction time are linear. This indicates that the loss rates of CH_3 at the wall of the reactor and in reaction 12 are negligible compared with the CH_3 consumption rate in reaction 2, at least at high initial concentrations of CH_3. Reaction 12 leads to the formation of another active species, H atoms. However, the possible impact of the secondary chemistry initiated by the H atoms on the CH_3 temporal profiles can be considered as negligible. Effectively, the concentrations of H atoms are low (as the concentrations of their precursor, O atoms, are low), and the possible reactions involving H atoms are slow under the experimental conditions used:

$$H + CH_3 (+M) \rightarrow CH_4 (+M) \qquad (18)$$

$$k_{18} = 6.2 \times 10^{-29}\ cm^6\ molecule^{-2}\ s^{-1}\ ^{22}$$

$$H + CH_4 \rightarrow H_2 + CH_3 \qquad (19)$$

$$k_{19} = 7.4 \times 10^{-19}\ cm^3\ molecule^{-1}\ s^{-1}\ ^{23}$$

Another potential secondary reaction which could influence the kinetics of CH_3 is the reaction of methyl radicals with F_2 (not dissociated in the discharge):

$$CH_3 + F_2 \rightarrow CH_3F + F \qquad (20)$$

$$k_{20} = 1.3 \times 10^{-12}\ cm^3\ molecule^{-1}\ s^{-1}\ ^{24}$$

However, the concentrations of F_2 remaining in the reactor are quite low (~90% is dissociated in the discharge), and F atoms formed in reaction 20 would regenerate CH_3 radicals through reaction 17.

The results obtained for k_2 at $P = 0.5$, 1.0, and 3.0 Torr are presented in Table 1. These data are shown also in Figure 10 along with those from previous studies of reaction 2 at $P < 10$ Torr. One can note a good agreement between our data and those of Slagle et al.[25] for M = He at a total pressure of 3 Torr. A similar pressure dependence of k_2 for He and Ar can be also observed from Figure 10, with somewhat lower values of k_2 for He than for Ar, as could be expected considering lower efficiency of He as third body.

Reactions of DMSO with CH_3 and Br_2. To better characterize the secondary chemistry which may occur in the study of reaction 1, reactions 3 and 4 of DMSO with CH_3 (major reaction product) and Br_2 (used to titrate CH_3), respectively, were studied.

For reaction 3, DMSO was introduced through inlet 2 and CH_3 radicals were generated in the same way as in the study of reaction 2. Br_2 added at the end of the reactor allowed for the detection of CH_3 as CH_3Br and O (from discharge of F_2) as BrO. Experiments were carried out in an excess of DMSO over CH_3 radicals ($[CH_3] \approx 2 \times 10^{11}$ molecule cm^{-3}). In the absence of DMSO, the observed consumption of CH_3 was due to reaction 2 and to a less extent to wall loss and reaction with oxygen atom traces present in the reactor. Introduction of DMSO ($1.1 \times 10^{12} - 2.7 \times 10^{13}$ molecule cm^{-3}) did not lead to an additional consumption of CH_3 radicals. On the contrary, a decrease of CH_3 decay rate was observed. This can be explained by the consumption of O atoms and formation of CH_3 in reaction 1 in the presence of DMSO. Thus, a simulation of the chemical system was needed in order to take into account reactions 1, 2, 3, and 12 occurring in the system. Finally, an upper limit for the rate constant of reaction 3 was derived:

$$k_3 < 1 \times 10^{-13}\ cm^3\ molecule^{-1}\ s^{-1}$$

The reaction between Br_2 and DMSO was studied using an excess of Br_2 (up to 5×10^{14} molecule cm^{-3}) injected by inlet 4, whereas DMSO (~10^{12} molecule cm^{-3}) was added through inlet 1. Flow velocity was near 800 cm s^{-1}. First, the wall loss of DMSO was observed in the absence of Br_2 in the reactor and the rate measured was (2.5 ± 0.5) s^{-1}. Addition of Br_2 did not lead to significant changes in the kinetics of DMSO. For the maximum concentration of Br_2 used, 5×10^{14} molecule cm^{-3}, the rate of DMSO consumption was found to be less than

4.2 s^{-1}. These data allowed to derive an upper limit for the rate constant of reaction 4

$$k_4 < 5 \times 10^{-15}\ cm^3\ molecule^{-1}\ s^{-1}$$

Discussion

Kinetics of reaction 1 between O atoms and DMSO has been investigated in only one previous study by Pope et al.,[12] where laser flash photolysis in combination with resonance fluorescence detection of O atoms was used to measure the reaction rate constant in the pressure range (20−100) Torr and temperatures between 266 and 383 K. The rate constant of reaction 1 was found to be independent of pressure and to increase with decreasing temperature. The room-temperature value of k_1 determined in ref 12, $k_1 = (7.5 \pm 2.2) \times 10^{-12}$ cm^3 $molecule^{-1}$ s^{-1}, can be compared with that from the present work: $k_1 = (1.0 \pm 0.2) \times 10^{-11}$ cm^3 $molecule^{-1}$ s^{-1} at $T = 298$ K and $P = 1$ Torr of He. One can note good agreement between these two values of k_1 obtained under different experimental conditions with different experimental techniques.

To our knowledge, no mechanistic study of the O + DMSO reaction has been reported previously. In the present work, the reaction channel 1a was shown to be the major if not unique one under the experimental conditions of the study:

$$O + CH_3S(O)CH_3 \rightarrow 2CH_3 + SO_2 \qquad (1a)$$

Reaction 1 proceeds most probably through the excited intermediate complex formation, $[DMSO_2]^*$, which may be stabilized or decompose with elimination of a methyl radical

$$O + CH_3S(O)CH_3 \leftrightarrow [CH_3S(O)(O)CH_3]^* \rightarrow CH_3S(O)(O)CH_3\ (+ M)$$
$$\rightarrow CH_3 + [CH_3SO_2]^*$$

The first channel is unlikely considering its high exothermicity (−112.7 kcal mol^{-1}[12]). In the second channel, the excited fragment $[CH_3SO_2]^*$ can lead to the following sequence of the processes:

$$[CH_3SO_2]^* \leftrightarrow CH_3 + SO_2$$
$$[CH_3SO_2]^* + M \leftrightarrow CH_3SO_2 + M$$
$$CH_3SO_2 + M \leftrightarrow CH_3 + SO_2 + M$$

Using simple thermochemical considerations, one can show that the first of these three reactions, i.e., excited CH_3SO_2 prompt decomposition, is the most probable. By definition, $\Delta H_f(CH_3SO_2) = \Delta H_f(CH_3) + \Delta H_f(SO_2) - BDE(CH_3-SO_2)$, where $BDE(CH_3-SO_2)$ is the CH_3-SO_2 bond dissociation energy. Then, using the known heat of formation data for CH_3, O,[13] and DMSO,[27] it is possible to express the enthalpy of the reaction

$$O + DMSO \rightarrow CH_3 + CH_3SO_2 \qquad (1b)$$

as a function of the bond dissociation energy of CH_3SO_2:

$$\Delta H_r = -(25 + BDE(CH_3-SO_2))\ kcal\ mol^{-1}$$

This last expression shows that the exothermicity of reaction 1b is 25 kcal mol^{-1} higher than the CH_3-SO_2 bond dissociation energy. Considering that the dissociation energy of CH_3SO_2 is near 14 kcal mol^{-1} [e.g., ref 11] and that at least a half of the energy released in reaction 1b is concentrated on CH_3SO_2, the most probable fate of $[CH_3SO_2]^*$ is expected to be its prompt decomposition.

It is interesting to compare this result with that obtained for the reaction of CH_3SO with NO_2.[11] This reaction has been suggested to proceed via the formation of the activated CH_3SO_2 radical, with only 20% of prompt decomposition (compared with 100% for the O + DMSO reaction) to CH_3 and SO_2 at 300 K and 1−600 Torr total pressure of helium. Applying to this reaction the same thermochemical calculation as above, one has $\Delta H_r = -((6.3 \pm 2.4) + BDE(CH_3-SO_2))$ kcal mol^{-1}. This calculation shows that the $CH_3SO + NO_2$ reaction is significantly less exothermic than reaction 1; that is, there is much less energy available for the CH_3SO_2 chemical activation−prompt decomposition in agreement with the experimental results. Therefore, the above discussion based on thermochemical consideration supports the experimental results suggesting that reaction 1a is predominant channel. Thermochemical consideration by Pope et al.[12] also led these authors to speculate that reaction 1 proceeds via channel 1a.

In conclusion, the mechanistic information obtained for reaction 1 in the present work shows that this reaction leads to the formation of two methyl radicals and SO_2 and cannot be used as a source of CH_3SO_2 in laboratory studies, at least at pressures around 1 Torr. Yet, this reaction can be used as a titration reaction for the in situ determination of the absolute concentrations of DMSO through detection of the stable product SO_2.

Acknowledgment. This study has been carried out within the EL CID project funded by the European Commission within the "Environment and Climate" Program.

References and Notes

(1) Charlson, J.; Lovelock, J. E.; Andreae, M. O.; Warren, S. G. *Nature* **1987**, *326*, 655.
(2) Berresheim, H.; Eisele, F. L.; Tanner, D. J.; McInnes, L. M.; Ramsey-Bell, D. C.; Covert, D. S. *J. Geophys. Res.* **1993**, *98*, 12701.
(3) Bandy, A. R.; Thornton, D. C.; Blomquist, B. W.; Chen, S.; Wade, T. P.; Ianni, J. C.; Mitchell, G. M.; Nadler, W. *Geophys. Res. Lett.* **1996**, *23*, 741.
(4) Berresheim, H.; Huey, J. W.; Thorn, R. P.; Eisele, F. L.; Tanner, D. J.; Jefferson, A. *J. Geophys. Res.* **1998**, *103*, 1629.
(5) Urbanski, S. P.; Wine, P. H. *S-Centered Radicals*; John Wiley & Sons Ltd.: New York, 1999.
(6) Barnes, I.; Becker, K. H.; Patroescu, I. V. *Atmos. Environ.* **1996**, *30*, 1805.
(7) Barnes, I.; Bastian, V.; Becker, K. H.; Overath, R. D. *Int. J. Chem. Kinet.* **1991**, *23*, 579.
(8) Bedjanian, Y.; Poulet, G.; Le Bras, G. *Int. J. Chem. Kinet.* **1996**, *28*, 383−389.
(9) Ingham, T.; Bauer, D.; Sander, R.; Crutzen, P. J.; Crowley, J. N. *J. Phys. Chem. A* **1999**, *103*, 7199.
(10) Urbanski, S. P.; Stickel, R. E.; Wine, P. H. *J. Phys. Chem. A* **1998**, *102*, 10522.
(11) Kukui, A.; Bossoutrot, V.; Laverdet, G.; Le Bras, G. *J. Phys. Chem. A* **2000**, *104*, 935.
(12) Pope, F. D.; Nicovich, J. M.; Wine, P. H. *Int. J. Chem. Kinet.* **2002**, *34*, 156.
(13) De More, W. B.; Sander, S. P.; Golden, D. M.; Hampson, R. F.; Kurylo, M. J.; Howard, C. J.; Ravishankara, A. R.; Kolb, C. E.; Molina, M. J. *Chemical Kinetics and Photochemical Data for Use in Stratospheric Modeling*; NASA, JPL, California Institute of Technology: Pasadena, CA, 1997.
(14) Nicovich, J. M.; Wine, P. H. *Int. J. Chem. Kinet.* **1990**, *22*, 379.
(15) James, F. C.; Kerr, J. A.; Simons, J. P. *Ber. Bunsen-Ges. Phys. Chem.* **1974**, *78*, 204.
(16) Fair, R. W.; Thrush, B. A. *Trans. Faraday Soc.* **1969**, *65*, 1550.
(17) Timonen, R. S.; Seetula, J. A.; Gutman, D. *J. Phys. Chem.* **1990**, *94*, 3005.
(18) Ballesteros, B.; Jensen, N. R.; Hjorth, J. *J. Atmos. Chem.* **2002**, *43*, 135.
(19) Kaufman, F. *J. Phys. Chem.* **1984**, *88*, 4909.

(20) Morrero, T. R.; Mason, E. A. *J. Phys. Chem. Ref. Data* **1972**, *1*, 3.
(21) Zelenov, V. V.; Kukuy, A. S.; Dodonov, A. F. *Sov. J. Chem. Phys*. **1990**, *5*, 1109.
(22) Baulch, D. L.; Cobos, C. J.; Cox, R. A.; Frank, P.; Hayman, G.; Just, Th.; Kerr, J. A.; Murrells, T.; Pilling, M. J.; Troe, J.; Walker, R. W.; Warnatz, J. *J. Phys. Chem. Ref. Data* **1994**, *23*, 847.
(23) Baulch, D. L.; Cobos, C. J.; Cox, R. A.; Esser, C.; Frank, P.; Just, Th.; Kerr, J. A.; Pilling, M. J.; Troe, J.; Walker, R. W.; Warnatz, J. *J. Phys. Chem. Ref. Data* **1992**, *21*, 411.
(24) Moore, C. M.; Smith, I. W. M.; Stewart, D. W. A. *Int. J. Chem. Kinet.* **1994**, *26*, 813.
(25) Slagle, I. R.; Gutman, D.; Davies, J. W.; Pilling, M. J. *J. Phys. Chem*. **1988**, *92*, 2455.
(26) Walter, D.; Grotheer, H.-H. *Symp. Int. Combust. Proc.* **1991**, *23*, 107.
(27) Masuda, N.; Nagano, Y.; Sakiyama, M. *J. Chem. Thermodyn*. **1994**, *26*, 971−975.